RING FAULTS ON SAPAS MONS (VENUS) AND ELLIPTICAL MAGMA CHAMBERS. D. W. vonLembke[1,2], S. T. O'Hara[1], P. J. McGovern[1], [1]Lunar and Planetary Institute/USRA, Houston, TX 77058, [2]Colorado School of Mines, Golden, CO 80401.

Introduction: The Sapas Mons volcano on Venus has an edifice radius of ~150 km and flow units extending more than 300 km from the summit [1, 2]. The summit is circumscribed by a series of extensional faults (graben) and fractures. These features (Fig. 1) may delineate the outer boundary of a subsurface magma chamber.

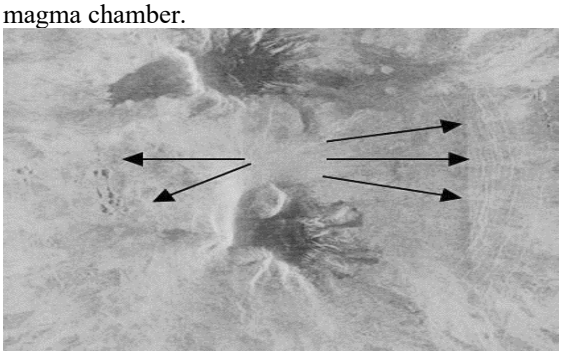

Figure 1: Magellan image of Sapas Mons [3]. The region shown is ~160 km on a side. Arrows indicate circumferential faults, fractures, and pit systems.

Gravitational loading and flexure for a volcanic edifice tends to produce compressional stresses near the summit, contrary to the extensional nature of these observed faults (Fig. 1). We are investigating how to model a stress state that is consistent with the observed graben without creating large enhanced compressional stresses elsewhere. To discover the conditions that lead to the observed faulting, we implemented models of the volcanic edifice in COMSOL Multiphysics.

Methods: In COMSOL we calculate stresses and strains in edifice-loaded elastic substrates using an axisymmetric geometry [e.g., 4-6]. The models consist of an edifice with initial (pre-deformation) radius 200 km and height 5 km plus an elliptical magma chamber with radius 50 km and height 2 km placed at various depths within the substrate. We apply a change in pressure normal to the chamber boundary to simulate withdrawal of magma from the chamber. Such changes are generally termed "overpressure", but we require negative values to simulate withdrawal so we use the term "underpressure".

The models calculate horizontal normal stresses in the plane of the model (σ_r, the "radial" stress) and perpendicular to the plane (σ_ϕ, the "hoop" stress) as well as the vertical normal stress σ_z. We use a tension-positive sign convention. We calculate differential stress σ_D as the difference between the greatest and least principal normal stresses. We also evaluate the "proximity to failure" (P_f) parameter, a measure of how close a given stress state is to failure according to a Mohr-Coulomb failure criterion: a value of 1 indicates that faulting is predicted at that location.

We investigate two types of substrates beneath the edifice. First, because a volcano the size of Sapas Mons would be expected to induce lithospheric flexure, we incorporate lithospheres of variable thickness T_e (20-50 km). Second, because models with flexure induce large amounts of horizontal compressive stress that may render it difficult to see signs of extensional stress at the surface, we also assess "half-space" models in which vertical deflections from loading and horizontal compressive stresses in the edifice remain small. The latter situation may correspond to cases in which the volcano is supported by dynamic forces in the mantle, related to plume upwellings.

Results and Discussion:

Half-space models. For half-space models, magma chamber deflation results in subsidence of the upper flank of the edifice, producing elevated values of σ_D and P_f above the chamber margin and also at the surface between the chamber margin and summit (Fig. 2).

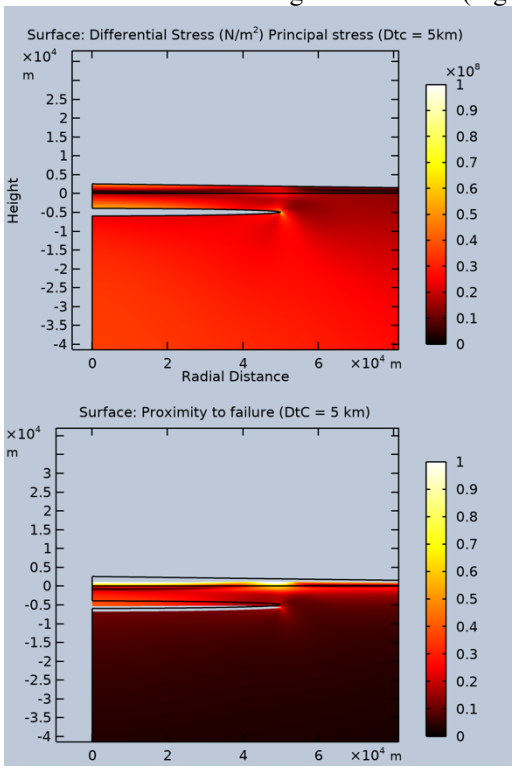

Figure 2. Cross-section of upper portion of the half-space model, with chamber 60 km radius and depth 5km. (a) Differential stress σ_D with a color scale of x10^8 Pa. (b) Proximity to failure (P_f), with original (outline) and deformed (color map) configurations.

In the half-space models, we adjusted the underpressure in order to achieve the following goals at the radial distance of the observed fractures: generation of 1) a local maximum in P_f, and 2) positive (extensional) values of σ_r. We also sought to minimize increases to the following quantities at other locations of the model: 3) horizontal compressive stresses, and 4) P_f. See Figures 2 and 3a for successful models.

In general the magnitude of underpressure required to produce predicted fracturing above the chamber edge increases with increasing depth of the chamber, similar to the way that increasing magnitudes of overpressure with increasing depth are required to achieve chamber wall failure, e.g., Fig. 10 of [4] , Fig. 6 of [7].

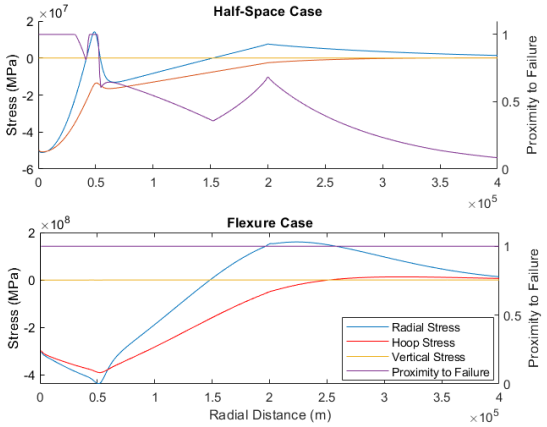

Figure 3: Normal stresses (σ_r, σ_ϕ, and σ_z) and proximity to failure (P_f) at edifice surface with chamber depth 5 km (a) for a half-space model. (b) for a flexure model with T_e = 40 km.

Flexure model. Models with chambers embedded in an edifice-loaded lithosphere ("flexure model") show high magnitudes of compressional stresses and P_f = 1 along the top of the instantaneously emplaced edifice (Fig 3b). Such conditions predict the formation of compressional faults covering the entire mid-flank to summit region, in contrast to the localized extensional features seen on Sapas Mons. One interesting departure from typical stress states for single-increment edifices [e.g., 8] is that the magnitudes of σ_r and σ_ϕ have an inflection point at about the radius of the chamber margin, such that they decrease toward the center rather than increase. This reflects the local bifurcation of the flexed lithosphere (comprising both the original underlying lithospheric plate and edifice) into two separate plates [e.g., 9] with differing responses based on their (disparate) thicknesses and basal loading profiles (flexural restoring forces for lower and chamber pressure for upper plate).

Model Evaluation. The half-space model is the most successful, and represents a case with minimal downward deflection (and resulting compressive stress) from loading, in contrast to the flexure case. This finding suggests that Sapas Mons currently benefits from flexure-offsetting topographic support, such as could result dynamically from the mantle plume magmatic source. Further, Sapas Mons appears to be emplaced atop a broader topographic swell, also consistent with mantle dynamic support.

Half-space models have enjoyed success in explaining the observed behaviors of intrusive and eruptive systems in numerous settings on Earth and other planets [e.g., 4, 10, 11]. It is clear that flexural substrate models with single-increment edifices are incapable of producing stress states consistent with observed extensional tectonic features on Sapas Mons (and many other edifices). However, edifices as large as Sapas Mons and Isla Fernandina [11] are expected to generate flexural responses to their emplacement, pointing to the need for more realistic edifice loading timescales to reduce the magnitudes of compressive stress at the surface [e.g., 8].

Future Directions: We have learned that magma chamber deformation can produce surface fractures akin to those seen on Sapas Mons, but only half-space models were capable of doing so. Our models to date use edifices that are emplaced as a single instantaneous load. We are working on flexural models with time dependent edifice emplacement (incremental growth) and will continue to examine the lithospheric bifurcation effect. We anticipate this will reduce the extreme compression seen at the edifice surface [8], thereby allowing creation of a stress state consistent with the observed fractures on Sapas Mons.

Acknowledgments: This material is based upon work supported by NASA through the Lunar and Planetary Institute (LPI) during the 2021 intern program, and also by NASA Grant 80NSSC18K0009 (SSW). The LPI is operated by Universities Space Research Association (USRA) under a cooperative agreement with the Science Mission Directorate of NASA.

References: [1] S.T. Keddie and J.W. Head (1994) Earth, Moon, and Planets, 65.2, 129-190. [2] P.J. McGovern and S.C. Solomon (1997) J. Geophys. Res. Planets 102.E7, 16303-16318. [3] Venus Magellan Global C3-MDIR Synthetic Color Mosaic 4641m v1, NASA PDS, 2014. [4] E. Grosfils (2007) J. Volcan. And Geotherm. Res., 166.2, 47-75; [5] G.A. Galgana et al. (2011) J. Geophys. Res. Planets, 166.E3 [6] N. Le Corvec et al. (2015) J. Geophys. Res. Planets 120.7, 1279-1297. [7] G.A. Galgana et al. (2013) Icarus, 255, 538-547. [8] McGovern and Solomon (1998) J. Geophys Res., 103, 11,071-11,101. [9] McGovern et al. (2001), J. Geophys. Res,,106, 23,769-23,809. [10] Hurwitz et al. (2009) JVGR, 188, 379-394. [11] Chestler and Grosfils (2013) GRL, 40, doi:10.1002/grl50833.